

PAPER • OPEN ACCESS

## Effect of Nb<sup>5+</sup> Doping on the Structure and Electrochemical Performances of LiFePO<sub>4</sub>

To cite this article: Lin Chen *et al* 2019 *IOP Conf. Ser.: Mater. Sci. Eng.* **493** 012045

View the [article online](#) for updates and enhancements.

You may also like

- [Nonstoichiometry in LiFe<sub>0.5</sub>Mn<sub>0.5</sub>PO<sub>4</sub>: Structural and Electrochemical Properties](#)  
Robin Amissé, Stéphane Hamelet, Darko Hanzel *et al.*
- [Structural Phase Formation and Tunable Luminescence of Eu<sup>2+</sup>-Activated Apatite-Type \(Ca,Sr,Ba\)<sub>5</sub>\(PO<sub>4</sub>\)<sub>3</sub>\(SiO<sub>4</sub>\)](#)  
Yanlin Huang, Jiahui Gan, Rui Zhu *et al.*
- [Doping Effect of Nb<sup>5+</sup> on the Microstructure and Defects of LiFePO<sub>4</sub>](#)  
Peixin Zhang, Yanyi Wang, Muchong Lin *et al.*



**ECS**  
The  
Electrochemical  
Society  
Advancing solid state &  
electrochemical science & technology

**DISCOVER**  
how sustainability  
intersects with  
electrochemistry & solid  
state science research

# Effect of Nb<sup>5+</sup> Doping on the Structure and Electrochemical Performances of LiFePO<sub>4</sub>

Lin Chen<sup>1,\*</sup>, Cheng Lu<sup>1</sup>, Shuo Yin<sup>2</sup>, Meng Wang<sup>1</sup>, Yiqiao Wang<sup>2</sup>, Hui Liu<sup>2</sup>,  
Yongzhi Ren<sup>2</sup>, Lingli Zuo<sup>1</sup>, Caiyu Guo<sup>1</sup>, Yang Zhang<sup>1</sup>, Yunbo Chen<sup>1</sup>

<sup>1</sup>Beijing National Innovation Institute of Lightweight Co. Ltd., Beijing 100083, China

<sup>2</sup>CNGR advanced material Co. Ltd., Guizhou 554300, China

\*Corresponding author e-mail: chenxxlin@126.com

**Abstract.** Nb-doped Li<sub>x</sub>Nb<sub>0.005</sub>Fe<sub>y</sub>PO<sub>4</sub>/C cathode material for lithium-ion batteries were prepared by two-fluid spray-drying using FePO<sub>4</sub>·2H<sub>2</sub>O, LiOH·H<sub>2</sub>O, C<sub>6</sub>H<sub>12</sub>O<sub>6</sub>(glucose) as raw materials under N<sub>2</sub> atmosphere. The effects of doping Nb<sup>5+</sup> on the structure, morphology and electrochemical performances of LiFePO<sub>4</sub> were investigated. The results show that Li<sub>x</sub>Nb<sub>0.005</sub>Fe<sub>y</sub>PO<sub>4</sub>/C has Olivine Structure and pure phase. The Li<sub>x</sub>Nb<sub>0.005</sub>Fe<sub>y</sub>PO<sub>4</sub>/C had an initial discharge specific capacity of 158.5mAh/g at 0.1C and its specific capacities were 109mAh/g at 5C. The initial charge/discharge efficiency reached 93.9%. The discharge specific capacity of the Li<sub>x</sub>Nb<sub>0.005</sub>Fe<sub>y</sub>PO<sub>4</sub>/C at 253K is 82.2mAh/g. This investigation suggests that the Nb<sup>5+</sup> doped material possess high rate capability and excellent low temperature electrochemical performance.

## 1. Introduction

As a cathode material for lithium ion batteries, LiFePO<sub>4</sub> is widely used because of its high specific capacity of 170mAh/g, rich resources, environmentally friendly, low price, good safety performance, reasonable cycle life and other advantages [1]. Meanwhile, LiFePO<sub>4</sub> is one of the anode materials in various applications such as electric power and batteries which need better performance of low temperature and the ratio of the corresponding requirement of the lithium iron phosphate material nano-particles. However, a main drawback of pristine LiFePO<sub>4</sub> is its very low intrinsic electronic conductivity ( $\sim 10^{-9}$  Scm<sup>-1</sup>), which results in less impressive performance at high rates and low temperature [2].

To solve this problem, various methods have been applied. Proper cation doping is one of the most effective ways to improve the electrical conductivity of LiFePO<sub>4</sub>, favoring fast charge and fast discharge rate [3]. Many researchers have reported that selective doping with Mg<sup>2+</sup>, Al<sup>3+</sup>, Ti<sup>4+</sup>, V<sup>5+</sup>, and W<sup>6+</sup> can greatly improve the kinetics of LiFePO<sub>4</sub> in terms of the capacity delivery, cycle life and rate capability [3–5].

In this work, Nb-doped Li<sub>x</sub>Nb<sub>0.005</sub>Fe<sub>y</sub>PO<sub>4</sub>/C cathode materials were synthesized to investigate the effect of Nb substitution on the electrochemical properties of LiFePO<sub>4</sub>/C.

## 2. Experiment

LiFePO<sub>4</sub>/C composite was synthesized by two-fluid spray drying using FePO<sub>4</sub>·2H<sub>2</sub>O, LiOH·H<sub>2</sub>O as raw materials and C<sub>6</sub>H<sub>12</sub>O<sub>6</sub> (glucose) as carbon sources. FePO<sub>4</sub>·H<sub>2</sub>O and LiOH·H<sub>2</sub>O were mixed with



a molar ratio of 1:1 and then glucose was added in. Next, the mixture was ground into powder which primary particle size was smaller than 200nm by wet ball-milling in aqueous solution. Then the precursor was dried via two-fluid spray drying. Finally, the precursor was sintered in the furnace with  $N_2$  gas at 350°C for 3h, and then at 700°C for 8h, and the  $LiFePO_4/C$  was obtained. The preparation steps of  $Li_xNb_{0.005}Fe_yPO_4/C$  were consistent with  $LiFePO_4/C$ , except that 0.5%  $Nb_2O_5$  was added when mixing.

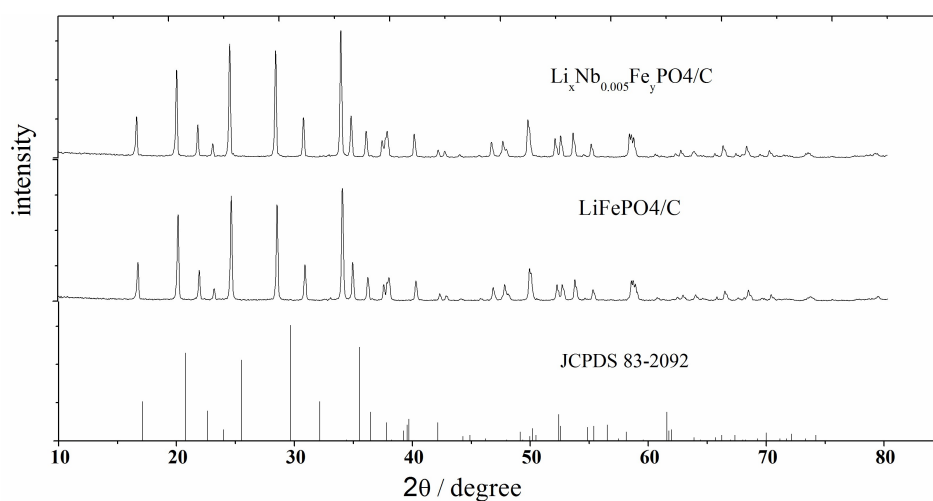
The electrodes were fabricated using a mixture of the prepared nano- $LiFePO_4/C$  powders (85wt. %), acetylene black (10wt. %), and polyvinylidene fluoride (PVDF 5wt. %) in N-methyl-2-pyrrolidone (NMP) to form a slurry. The slurry was spread onto Al foil and dried in an oven at 110°C under vacuum. The thickness of the electrode was 20 $\mu$ m or so. The electrochemical performance was tested by coin cells, using Li metal as the negative electrode and Celguard 2400 as the separator. The electrolyte solution was 1mol/L  $LiPF_6$  in a 1:1:1(volume ratio) mixture of ethylene carbonate, dimethyl carbonate and ethylene methyl carbonate. The charge-discharge test was performed on the LAND test system between the voltage limits of 2.5V and 4.2V (versus  $Li/Li^+$ ).

The structure and phase were identified by Rigaku D/MAX 2500PC X-ray diffraction (XRD) using  $Cu-K\alpha$  radiation, 30KV tube voltage. The morphology of the as-prepared products was characterized by scanning electron microscope (SEM). The particle size distributions were measured with laser scattering techniques (BT-9300, China and Horiba LA-950, Japan). The surface area was calculated using the Brunauer–Emmett–Teller (BET) equation (F-sorb2400, China). The tap density was measured by tap density tester (ZS-201, China).

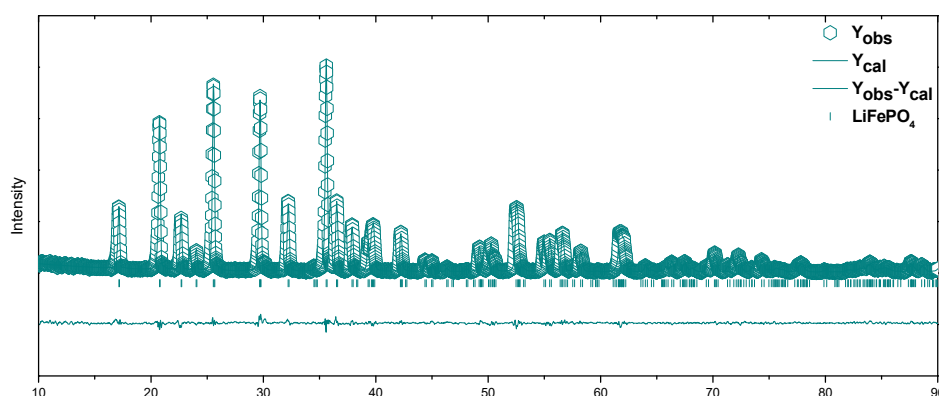
### 3. Results and discussion

Fig.1 shows the X-ray diffraction (XRD) patterns of the  $LiFePO_4/C$  and  $Li_xNb_{0.005}Fe_yPO_4/C$ . As seen, the synthesized  $LiFePO_4/C$  and  $Li_xNb_{0.005}Fe_yPO_4/C$  has a good crystallization from the shape of diffraction peaks which are sharp and has an ordered olivine-type indexed by orthorhombic Pnma (JCPDS No.83–2092). Besides, there are no obvious carbon diffraction peaks in the samples due to its low content and amorphous state.

The Rietveld refinements allowed the determination of the lattice and structural parameters. The profile parameters of the pseudo-Voigt function were used to describe the shape of the diffraction lines and the structural refinement was carried out by considering the [Li] 4a [Fe] 4cPO4 structural hypothesis [6]. In order to further investigate the occupancy of  $Nb^{5+}$  in  $LiFePO_4$  structure, XRD test results of doped sample were refined. Fig.2 exhibits comparison of the experimental and calculated XRD patterns of  $Li_xNb_{0.005}Fe_yPO_4/C$ . The hexagon symbol represents the experimental test value, and the baseline at the bottom is the difference between the actual test value and the calculated value. The observed pattern and calculated pattern match well in this case, and the agreement factors are satisfactory ( $R_{wp} = 13.5\%$ ,  $R_p = 9.8\%$ ). According to the results of the refinement, the doped sample with 0.5%  $Nb^{5+}$  can be expressed as  $(Li_{0.98788}Nb_{0.005}Fe_{0.00712})_{Li}(Fe_{0.99228}Li_{0.00712})_{Fe}PO_4$ .  $Nb^{5+}$  is mainly occupied in the Li position in the lattice, and a small amount of Fe exists in the Li position.



**Fig.1** The XRD patterns of LiFePO<sub>4</sub>/C and Li<sub>x</sub>Nb<sub>0.005</sub>Fe<sub>y</sub>PO<sub>4</sub>/C samples



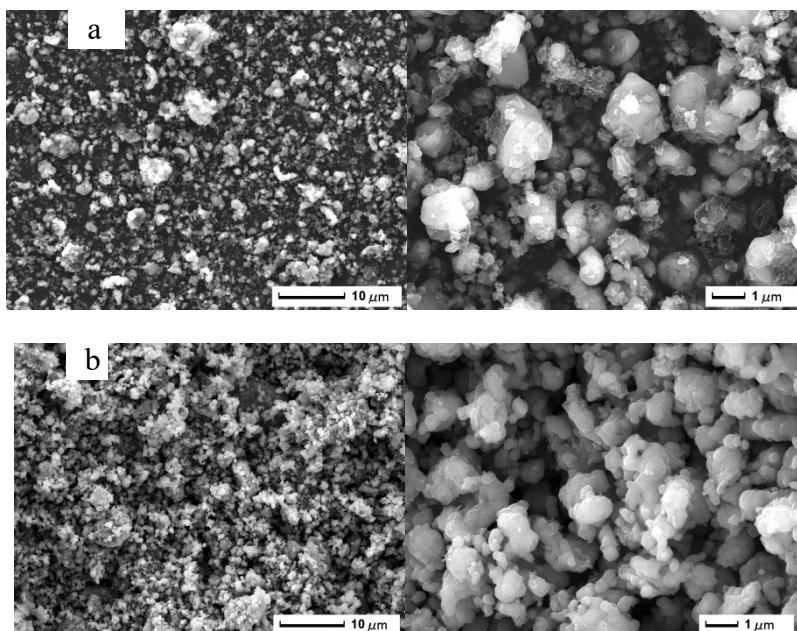
**Fig.2** Comparison of the experimental and calculated XRD patterns of Li<sub>x</sub>Nb<sub>0.005</sub>Fe<sub>y</sub>PO<sub>4</sub>/C

Fig.3 exhibits SEM images of the LiFePO<sub>4</sub>/C and Li<sub>x</sub>Nb<sub>0.005</sub>Fe<sub>y</sub>PO<sub>4</sub>/C samples. The particles of the LiFePO<sub>4</sub>/C and Li<sub>x</sub>Nb<sub>0.005</sub>Fe<sub>y</sub>PO<sub>4</sub>/C are small, well-dispersed, and no agglomerations exist. The particle size of Li<sub>x</sub>Nb<sub>0.005</sub>Fe<sub>y</sub>PO<sub>4</sub>/C particle is smaller than that of LiFePO<sub>4</sub>/C particle, and the primary grain is more uniform. This is due to the fact that Nb<sub>2</sub>O<sub>5</sub> powder may be used as nucleating agent in the sintering process, which has the effect of grain refinement. In addition, the particle size distributions for the aggregated particle size and primary particle size are given in Fig.4. From the images, we can acquire that particles of LiFePO<sub>4</sub>/C and Li<sub>x</sub>Nb<sub>0.005</sub>Fe<sub>y</sub>PO<sub>4</sub>/C are uniform with aggregated average particle size is 6.66 and 5.28 μm, respectively. The primary average particle size of Li<sub>x</sub>Nb<sub>0.005</sub>Fe<sub>y</sub>PO<sub>4</sub>/C is 132nm. It's more beneficial to shorten the internal migration distance of the Li-ions and electrons, reduce the ionic diffusion resistance and more effectively improve the contact with the electrolyte, the specific capacity and ratio discharge property.

Table 1 exhibits particle size distribution, apparent density, tap density and special BET surface of LiFePO<sub>4</sub>/C and Li<sub>x</sub>Nb<sub>0.005</sub>Fe<sub>y</sub>PO<sub>4</sub>/C samples. The measured apparent density of Li<sub>x</sub>Nb<sub>0.005</sub>Fe<sub>y</sub>PO<sub>4</sub>/C is 0.65g/cm<sup>3</sup> and the measured tap density is 0.93g/cm<sup>3</sup>. The special BET surface of the synthesized LiFePO<sub>4</sub>/C and Li<sub>x</sub>Nb<sub>0.005</sub>Fe<sub>y</sub>PO<sub>4</sub>/C is 14.97 and 13.88 m<sup>2</sup>/g. This lower BET surface of Li<sub>x</sub>Nb<sub>0.005</sub>Fe<sub>y</sub>PO<sub>4</sub>/C can improve the processing performance of the lithium batteries.

Fig.5 exhibits the initial charge and discharge curves of LiFePO<sub>4</sub>/C and Li<sub>x</sub>Nb<sub>0.005</sub>Fe<sub>y</sub>PO<sub>4</sub>/C at rate of 0.1C and 0.5C. The initial discharge capacity of the LiFePO<sub>4</sub>/C and Li<sub>x</sub>Nb<sub>0.005</sub>Fe<sub>y</sub>PO<sub>4</sub>/C are 160.2 and 158.5mAh/g at 0.1C, with the first discharge efficiency are 94.4% and 93.9%, respectively. The characteristic of extremely flat cell reaction voltage of two samples is observed here also. The charge

platform voltage of two samples is 3.44V and the discharge platform voltage of  $\text{LiFePO}_4/\text{C}$  and  $\text{Li}_x\text{Nb}_{0.005}\text{Fe}_y\text{PO}_4/\text{C}$



**Fig.3** SEM images of the  $\text{LiFePO}_4/\text{C}$  and  $\text{Li}_x\text{Nb}_{0.005}\text{Fe}_y\text{PO}_4/\text{C}$  samples(a:  $\text{LiFePO}_4/\text{C}$ , b:  $\text{Li}_x\text{Nb}_{0.005}\text{Fe}_y\text{PO}_4/\text{C}$ )

**Tab.1** Particle size, density and the special surface area of the samples

Simple	Particle size( $\mu\text{m}$ )			Apparent density ( $\text{g}/\text{cm}^3$ )	Tap density ( $\text{g}/\text{cm}^3$ )	Specific surface area ( $\text{m}^2/\text{g}$ )
	D10	D50	D90			
$\text{LiFePO}_4/\text{C}$	0.90	6.66	23.89	0.88	1.09	14.97
$\text{Li}_x\text{Nb}_{0.005}\text{Fe}_y\text{PO}_4/\text{C}$	0.83	5.28	22.42	0.65	0.93	13.88

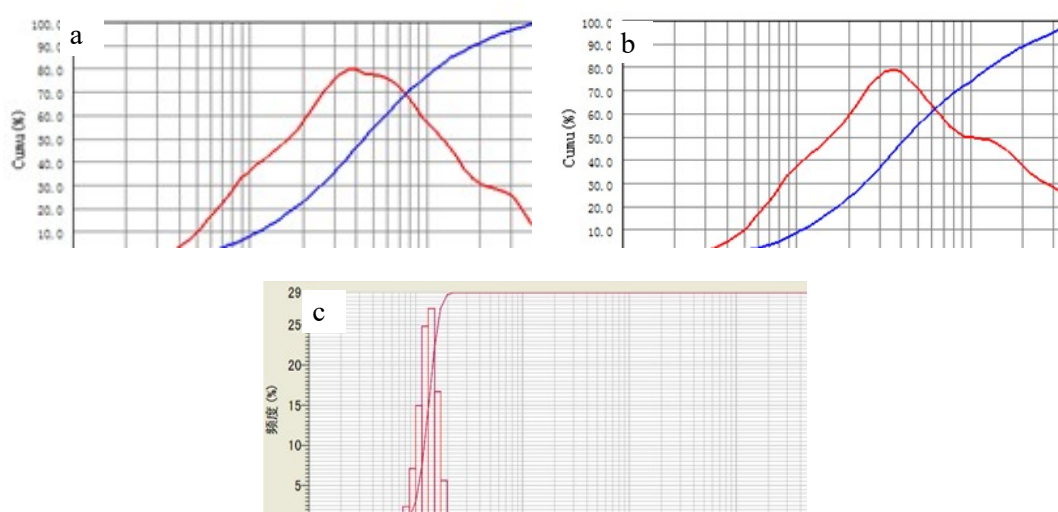


**Fig.4** Particle size distribution curves of  $\text{LiFePO}_4$  for the aggregated particle (a) and  $\text{Li}_x\text{Nb}_{0.005}\text{Fe}_y\text{PO}_4/\text{C}$  for the aggregated particle (b) and primary particle (c)

Is 3.39V and 3.38V. The difference between the charging and discharging voltage is only 50mv ( $\text{LiFePO}_4/\text{C}$ ) and 60mv ( $\text{Li}_x\text{Nb}_{0.005}\text{Fe}_y\text{PO}_4/\text{C}$ ) at 0.1 C, indicating very low electrode resistance and good kinetics of redox reaction at comparatively low discharge currents. Fig.5 (b) shows that the initial discharge capacity of the  $\text{LiFePO}_4/\text{C}$  and  $\text{Li}_x\text{Nb}_{0.005}\text{Fe}_y\text{PO}_4/\text{C}$  are 146.7 and 144.9mAh/g at 0.5C. The specific capacity of  $\text{Li}_x\text{Nb}_{0.005}\text{Fe}_y\text{PO}_4/\text{C}$  is slightly smaller than that of  $\text{LiFePO}_4/\text{C}$  at low discharge currents.

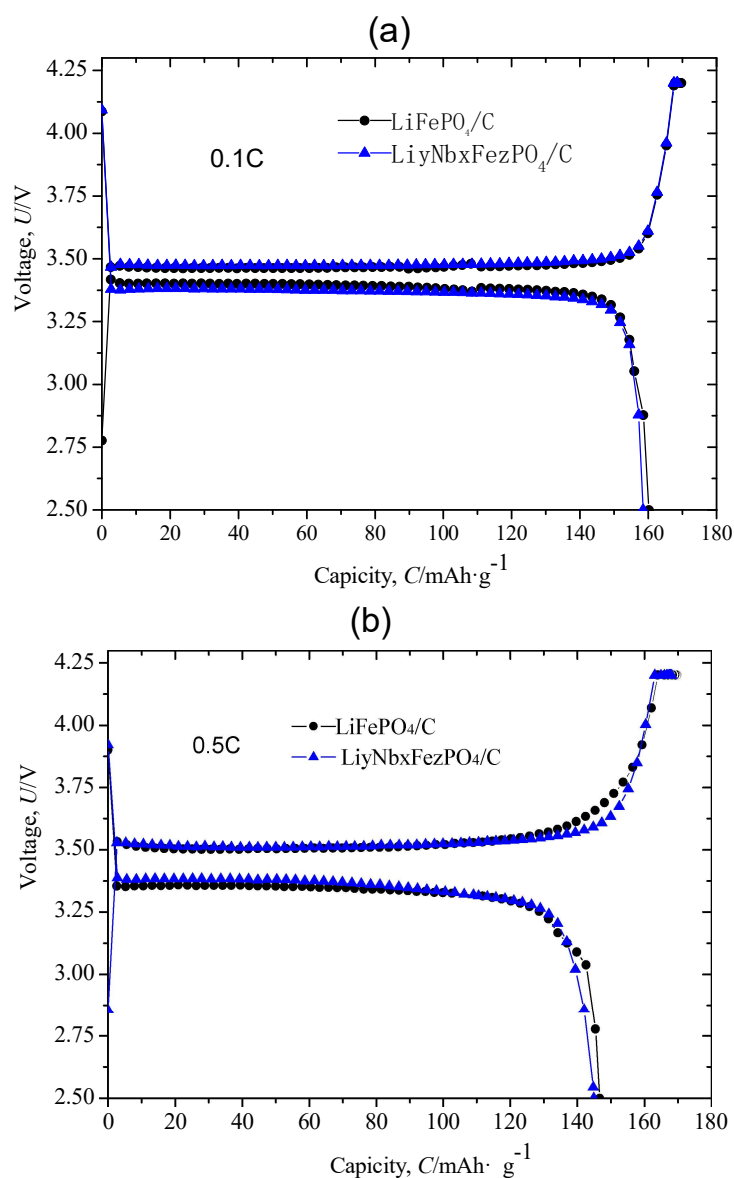


**Fig.5** Initial charge and discharge curves of  $\text{LiFePO}_4/\text{C}$  and  $\text{Li}_x\text{Nb}_{0.005}\text{Fe}_y\text{PO}_4/\text{C}$  at 0.1C (a) and 0.5C (b)

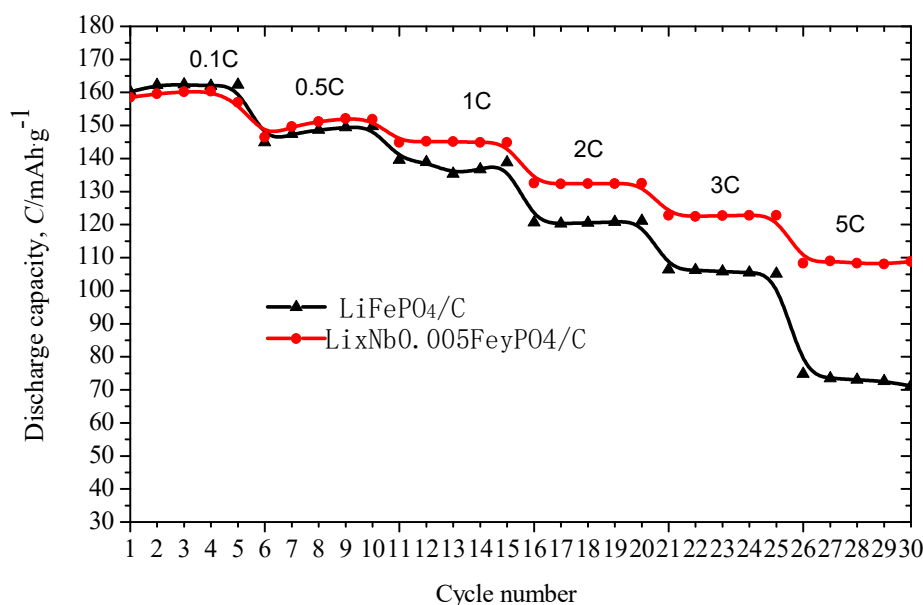


**Fig.6** Cycle curves at different current rates of  $\text{LiFePO}_4/\text{C}$  and  $\text{Li}_x\text{Nb}_{0.005}\text{Fe}_y\text{PO}_4/\text{C}$  samples

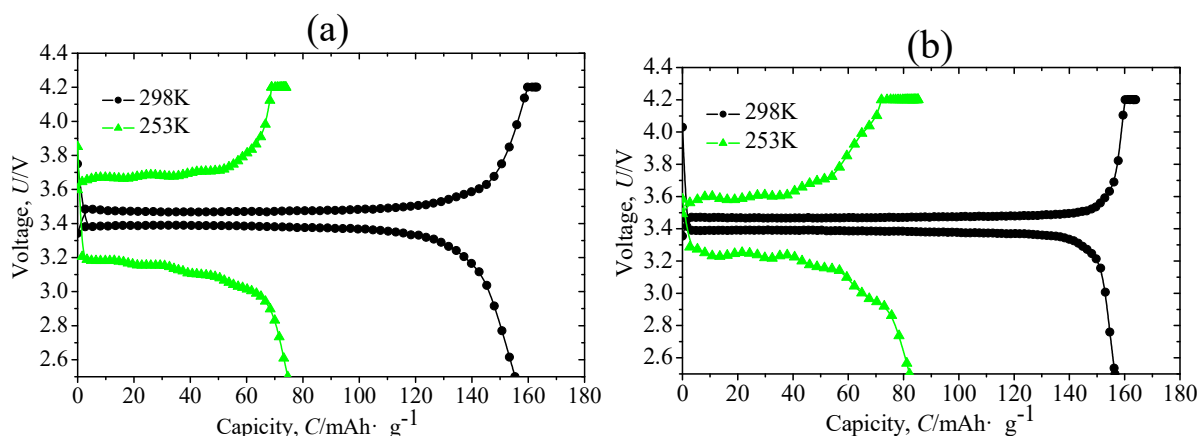


**Fig.7** Charge and discharge curves of samples at different temperature with 0.2C(a:  $\text{LiFePO}_4/\text{C}$ , b:  $\text{Li}_x\text{Nb}_{0.005}\text{Fe}_y\text{PO}_4/\text{C}$ )

With an increase in C-rate, polarization is enhanced due to slow lithium ion diffusion at the solid, two-phase  $\text{FePO}_4/\text{LiFePO}_4$  interface and the resulting limitation of the material to cope up with the fast reaction kinetics at high C-rates. Fig.6 exhibits the cycle curves of two samples at different current rates. The results are shown that the discharge capacity of  $\text{LiFePO}_4/\text{C}$  at 0.1C, 0.5C, 1C, 2C, 3C and 5C respectively reached 162.4, 149.8, 139.6, 121.1, 106.4, 74.8mAh/g, and the discharge capacity of  $\text{Li}_x\text{Nb}_{0.005}\text{Fe}_y\text{PO}_4/\text{C}$  reached 160.4, 152.1, 144.2, 132.6, 122.8 and 109.0mAh/g. It can be clearly seen that the specific capacity of undoped sample is slightly higher than that of doped sample at low discharge currents, but the specific capacity of undoped sample decreases significantly with the increase of the ratio, while that of doped sample decreases less. The difference between the specific capacity of undoped and doped samples increases with the increase of the ratio. The lower specific capacity of the doped sample may be due to the fact that  $\text{Nb}^{5+}$  doping occupies the Li site, resulting in the reduction of the amount of decanted Li, which can also be explained by Nb occupying Li site in

lithium iron phosphate. However,  $\text{Nb}^{5+}$  doping can effectively improve the conductivity and diffusion rate of lithium ions, thus obviously improving high rate capability.

Fig.7 exhibits charge and discharge curves of  $\text{LiFePO}_4/\text{C}$  and  $\text{Li}_x\text{Nb}_{0.005}\text{Fe}_y\text{PO}_4/\text{C}$  at 253K and 298K with 0.2C. The results are shown that the discharge capacity of undoped sample reached 155.3mAh/g at 298K and 74.6mAh/g at 253K with 0.2C. Under low temperature 253K, the discharge capacity is 48.0% of that at 298K. The discharge capacity of doped sample reached 156.5mAh/g at 298K and 82.2mAh/g at 253K with 0.2C. Under low temperature 253K, the discharge capacity is 52.2% of that at 298K, suggesting that the doped sample has better low temperature electrochemical performance.

#### 4. Conclusion

Nb-doped  $\text{Li}_x\text{Nb}_{0.005}\text{Fe}_y\text{PO}_4/\text{C}$  cathode material for lithium-ion batteries is synthesized by two-fluid spray-drying. Through the Rietveld refinement from XRD data, it is shown that  $\text{Nb}^{5+}$  is mainly occupied in the Li position in the lattice, and a small amount of Fe exists in the Li position. Compared with undoped  $\text{LiFePO}_4/\text{C}$ , the Nb-doped  $\text{Li}_x\text{Nb}_{0.005}\text{Fe}_y\text{PO}_4/\text{C}$  has better high rate capability and low temperature electrochemical performance. It can meet the requirements for high power applications such as electric vehicle, electric tool and energy storage for smart power grids.

#### Acknowledgments

This work was supported by 863 program (2012AA052203), Natural Science Foundation of China (51202083).

#### References

- [1] L.X. Yuan, Z.H. Wang, W.X. Zhang, X.L. Hu, et al. Development and challenges of  $\text{LiFePO}_4$  cathode material for lithium-ion batteries, *J. Energy & Environmental Science*. 4 (2011) 269-284.
- [2] Y.J Gu, C.J Li, et al. Novel Synthesis of Plate-like  $\text{LiFePO}_4$  by Hydrothermal Method. *Journal of New Materials for Electrochemical Systems*, 19(2016)33-36.
- [3] S.I. Nishimura, G. Kobayashi, K. Ohoyama, R. Kanno, M. Yashima, A. Yamada, *Nat. Mater.* 7 (2008) 707.
- [4] C.S. Sun, Z. Zhou, Z.G. Xu, D.G. Wang, J.P. Wei, X.K. Bian, J. Yan, *J. Power Sources* 193 (2009) 841.
- [5] Y. Wang, Y. Yang, X. Hu, Y. Yang, H. Shao, *J. Alloys Compd.* 481 (2009) 590.
- [6] Carmen Parada, Carlos Garcia Giron, et al. Synthesis and characterization of  $\text{LiFePO}_4/\text{C}$  nanocomposites. *Physics Procedia* 8 (2010) 33–38.